

X-RAY OBSERVATIONS OF XSS J12270–4859 IN A NEW LOW STATE: A TRANSFORMATION TO A DISK-FREE ROTATION-POWERED PULSAR BINARY

SLAVKO BOGDANOV¹, ALESSANDRO PATRUNO^{2,3}, ANNE M. ARCHIBALD³, CEES BASSA³,
JASON W. T. HESSELS^{3,4}, GEMMA H. JANSSEN³, BEN W. STAPPERS⁵

Draft version March 3, 2018

ABSTRACT

We present *XMM-Newton* and *Chandra* observations of the low-mass X-ray binary XSS J12270–4859, which experienced a dramatic decline in optical/X-ray brightness at the end of 2012, indicative of the disappearance of its accretion disk. In this new state, the system exhibits previously absent orbital-phase-dependent, large-amplitude X-ray modulations with a decline in flux at superior conjunction. The X-ray emission remains predominantly non-thermal but with an order of magnitude lower mean luminosity and significantly harder spectrum relative to the previous high flux state. This phenomenology is identical to the behavior of the radio millisecond pulsar binary PSR J1023+0038 in the absence of an accretion disk, where the X-ray emission is produced in an intra-binary shock driven by the pulsar wind. This further demonstrates that XSS J12270–4859 no longer has an accretion disk and has transformed to a full-fledged eclipsing “redback” system that hosts an active rotation-powered millisecond pulsar. There is no evidence for diffuse X-ray emission associated with the binary that may arise due to outflows or a wind nebula. An extended source situated 1.5′ from XSS J12270–4859 is unlikely to be associated, and is probably a previously uncatalogued galaxy cluster.

Subject headings: pulsars: general — pulsars: individual (XSS J12270–4859) — stars: neutron — X-rays: binaries

1. INTRODUCTION

Since the original discovery of millisecond pulsars (MSPs; Backer et al. 1982) the prevailing theory of their formation has centered on “recycling” by transfer of matter and angular momentum from a close companion star during a low-mass X-ray binary (LMXB) phase (Alpar et al. 1982; Radhakrishnan & Srinivasan 1982). The discovery of the first accreting X-ray MSP, SAX J1808.4–3658 (Wijnands & van der Klis 1998), provided compelling evidence for this evolutionary sequence (see also Patruno & Watts 2012, for a review). Additional observational support in favor of this hypothesis came with the discovery of the “missing link” radio pulsar PSR J1023+0038 (also known as FIRST J102347.6+003841). Optical observations revealed an accretion disk in the system in 2001 (Wang et al. 2009), which was absent after 2003 (Thorstensen & Armstrong 2005) and at the time of the radio pulsar discovery in 2009 (Archibald et al. 2009). The long-suspected evolutionary connection between LXMBs and radio MSPs was conclusively established when PSR J1824–2452I in the globular cluster M28 was seen to switch between rotation-powered (radio) and high-luminosity accretion-powered (X-ray) pulsations (Papitto et al. 2013).

Recent radio, X-ray, and γ -ray observations revealed that in 2013 June PSR J1023+0038 had undergone another transformation (Stappers et al. 2014). Complete cessation of radio pulsations was observed, accompanied by an extraordinary five-fold increase in the *Fermi* Large Area Telescope (LAT) flux and enhancement in UV and X-ray brightness (Patruno et al. 2014; Tendulkar et al. 2014). These recent findings have revealed that rather than a one-time change from a LMXB to a permanent radio MSP state, for some systems this phase of neutron star compact binary evolution involves recurrent switching between the two states.

In the absence of an accretion disk, PSRs J1023+0038 and PSR J1824–2452I belong to the family of so-called “redbacks” (see Roberts 2011, and references therein), namely, eclipsing radio MSPs with relatively massive ($\gtrsim 0.2 M_{\odot}$) non-degenerate companions that are (nearly) Roche-lobe filling. These objects are distinct from “black widow” systems, which are bound to very low mass degenerate stars being ablated by the pulsar wind (Fruchter et al. 1988; Stappers et al. 1996). Extensive X-ray studies of redbacks in globular clusters (Bogdanov et al. 2005, 2010, 2011b) and the field of the Galaxy (Archibald et al. 2010; Bogdanov et al. 2011a, 2014; Gentile et al. 2014) have revealed that the dominant source of X-rays from these binaries is non-thermal radiation with $\Gamma \approx 1 - 1.5$ originating in an intra-binary shock (Arons & Tavani 1993) generated by the interaction of the pulsar wind and matter from the companion star. The X-ray emission is strongly modulated at the orbital period in all redback systems, with a decline in flux when the secondary star is between the pulsar and the observer. This orbital-phase-dependent X-ray variability appears to be a distinguishing characteristic of these peculiar MSP binaries and provides a convenient way to identify additional redbacks even in the absence

¹ Columbia Astrophysics Laboratory, Columbia University, 550 West 120th Street, New York, NY 10027, USA; slayko@astro.columbia.edu

² Leiden Observatory, Leiden University, PO Box 9513, 2300 RA, Leiden, The Netherlands

³ ASTRON, the Netherlands Institute for Radio Astronomy, Postbus 2, 7990 AA, Dwingeloo, The Netherlands

⁴ Anton Pannekoek Institute for Astronomy, University of Amsterdam, Science Park 904, 1098 XH Amsterdam, The Netherlands

⁵ Jodrell Bank Centre for Astrophysics, School of Physics and Astronomy, The University of Manchester, Manchester M13 9PL, UK

of radio pulsations.

The Galactic X-ray source XSS J12270–4859 (1RXS J122758.8–485343) has posed a mystery since its discovery. Although initially classified as a cataclysmic variable (Masetti et al. 2006; Butters et al. 2008), subsequent multi-wavelength studies (Pretorius 2009; de Martino et al. 2010; Hill et al. 2011; de Martino et al. 2013; Papitto et al. 2014) revealed that this system closely resembles a quiescent LMXB. XSS J12270–4859 is exceptional in that it was the first LMXB putatively associated with a γ -ray source, 1FGL J1227.9–4852 (Hill et al. 2011), now known as 2FGL J1227.7–4853 (Nolan et al. 2012). Deep searches have failed to detect radio pulsation from XSS J12270–4859 during its high optical/X-ray flux state (Hill et al. 2011).

Prior to 2012 November/December, the X-ray spectrum of XSS J12270–4859 was well described by a pure powerlaw with $\Gamma = 1.7$ and a 0.1–10 keV luminosity of $\sim 6 \times 10^{33}$ erg s $^{-1}$ (de Martino et al. 2010, 2013). The source exhibited occasional intense flares and peculiar, frequent drops in X-ray flux that are not correlated with orbital phase. This behavior is reminiscent of the erratic flux variations observed in PSRs J1023+0038 (Patruno et al. 2014; Tendulkar et al. 2014; S. Bogdanov in prep.) and J1824–2452I (Papitto et al. 2013; Linares et al. 2014) in their accretion disk states, hinting at a connection with these systems. Recent optical and X-ray observations revealed that XSS J12270–4859 had undergone a substantial decline in brightness and no longer exhibits evidence for an accretion disk (Bassa et al. 2014). The abrupt change to a disk-free system appears to have occurred between 2012 November 14 and 2012 December 21. Given the similarities with PSR J1023+0038 in both states, XSS J12270–4859 is presently consistent with hosting a rotation-powered millisecond pulsar. This prediction was confirmed with the recent detection of 1.69-millisecond radio pulsations from the system (Roy et al. 2014).

Here we present recently acquired *XMM-Newton* European Photon Imaging Camera (EPIC) and *Chandra X-ray Observatory* Advanced CCD Imaging Spectrometer (ACIS) observations of XSS J12270–4859 in its new low flux state. These observations confirm that this source has undergone a metamorphosis to a redback, i.e. a compact binary containing a rotation-powered millisecond pulsar. The analysis is presented as follows. In §2, we provide details on the observations and data reduction procedures. In §3, we present an X-ray variability study. In §4 we summarize the phase-averaged and phase-resolved spectroscopy, while in §5 we report on an imaging analysis. We provide a discussion and conclusions in §6.

2. OBSERVATIONS AND DATA REDUCTION

2.1. *XMM-Newton* EPIC

Motivated by the sudden decline in X-ray and optical brightness of XSS J12270–4859 (Bassa et al. 2014), we obtained a target of opportunity *XMM-Newton* observation on 2013 December 29 (ObsID 0727961401) for a total exposure time of 38-ks. The pn (Strüder et al. 2001) and two MOS (Turner et al. 2001) EPIC instruments used the thin optical blocking filters and were set up in Full Window mode. The data were processed us-

ing the *XMM-Newton* Science Analysis Software (SAS⁶) version `xmmsas_20130501_1901-13.0.0`. After applying the recommended flag, pattern, and pulse invariant filters, the event lists were screened for instances of strong background flares, which resulted in effective exposures of 31.2, 31.2, and 26.9 ks for the MOS1, MOS2, and pn, respectively.

For the variability and spectral analyses presented in §3 and §4, source counts were extracted from each detector within a circular region of radius 40'', which contains $\sim 90\%$ of the point source energy. The background counts were extracted from three source-free regions on the same detector chip as the target. To study the system's X-ray variability, the photon arrival times were barycentred using the `barycen` SAS command with the DE405 solar system ephemeris and assuming the source J2000 coordinates RA=12^h27^m58^s.748, Dec=−48°53′42″88. Owing to the coarse read-out time of the EPIC instruments in Full Window mode (0.73 s and 2.6 s for the pn and MOS, respectively), it was not possible to search for pulsations in the millisecond range.

The simultaneous fast photometry U band filter data obtained with the *XMM-Newton* Optical Monitor (OM) were presented in Bassa et al. (2014).

2.2. *Chandra* ACIS-S

To look for extended emission around XSS J12270–4859, a target of opportunity *Chandra* ACIS-S observation was conducted on 2014 January 11 (ObsID 16561) for a duration of 30.2-ks. The best known position of XSS J12270–4859 was placed at the nominal aim point of the ACIS S3 chip, which was configured in FAINT telemetry mode. The data processing and analysis were performed with CIAO⁷ 4.6 (Fruscione et al. 2006) and CALDB 4.5.9 using standard procedures.

For the variability and spectroscopic studies, we extracted photons within 2'' of the source. For the variability study the event times were translated to the solar system barycenter assuming the DE405 JPL solar system ephemeris and the same position for XSS J12270–4859 used for the *XMM-Newton* data. The 3.2-s read-out for ACIS-S prevented a search for pulsations. To produce spectra suitable for analysis, the extracted source counts in the 0.3–8 keV range were grouped so as to ensure at least 15 counts per energy bin. The background was taken from three source-free circular regions near the target.

3. X-RAY ORBITAL VARIABILITY

Based on the refined binary orbital period ($P_b = 6.913 \pm 0.002$ hours) and reference epoch of the ascending node (HJD 2456651.026 \pm 0.002 corresponding to orbital phase $\phi_b = 0$) of XSS J12270–4859 obtained in Bassa et al. (2014) we have folded the barycentered *XMM-Newton* and *Chandra* point source X-rays at the binary period. Both observations span slightly more than one binary orbit. Large-amplitude variability correlated with binary phase is immediately evident from Figure 1.

⁶ The *XMM-Newton* SAS is developed and maintained by the Science Operations Centre at the European Space Astronomy Centre and the Survey Science Centre at the University of Leicester.

⁷ *Chandra* Interactive Analysis of Observations, available at <http://cxc.harvard.edu/ciao/>.

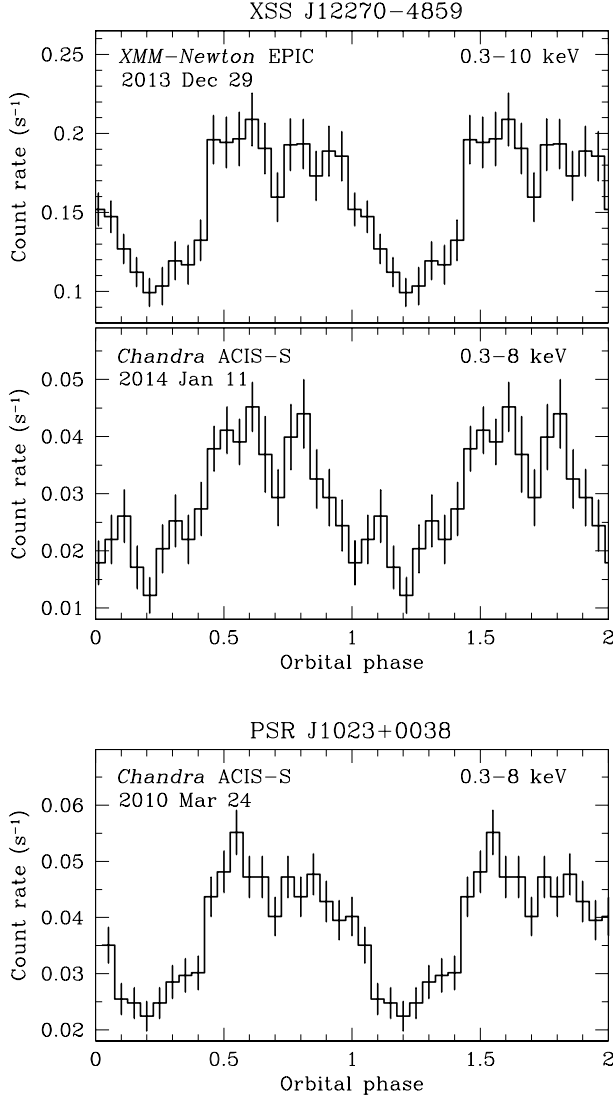


FIG. 1.— Exposure-corrected, background-subtracted lightcurves of XSS J12270–4859 from *XMM-Newton* EPIC (*top*) and *Chandra* ACIS-S (*middle*) observations. In both cases, the data are folded using the binary orbital ephemeris determined in Bassa et al. (2014). For comparison, the bottom panel shows the folded *Chandra* ACIS-S data of PSR J1023+0038 in the disk-free radio pulsar state. Two orbital cycles are shown for clarity.

This behavior is in stark contrast with the *XMM-Newton* observations from 2009 and 2011 (de Martino et al. 2010, 2013) where no orbital dependence on the X-ray flux is seen and only random, aperiodic variability is present. To formally establish the statistical significance of the variability, we use a Kuiper test (Paltani 2004), which accounts for the non-uniform exposure across the orbit of the folded lightcurves and is not dependent on the choice of binning of the lightcurve, making it a better-suited choice than the Kolmogorov-Smirnov and χ^2 tests for this purpose. Applying this test to the folded, unbinned lightcurves, yields 7×10^{-41} (13.3σ) and 7×10^{-15} (7.7σ) probabilities for the *XMM-Newton* and *Chandra* data, respectively, that photons drawn from a constant distribution would exhibit this level of non-uniformity.

For comparison, the folded lightcurve of PSR

TABLE 1
RESULTS OF JOINT *XMM-Newton*/*Chandra* SPECTRAL FITS
FOR XSS J12270–4859.

Model ^a	Total	$\phi_{b,1}$ (0.0 – 0.5)	$\phi_{b,2}$ (0.5 – 1.0)
PL			
N_H (10^{20} cm^{-2})	6.1 ± 1.1	$3.6^{+1.6}_{-1.5}$	$5.2^{+0.9}_{-0.5}$
Γ	1.20 ± 0.04	1.19 ± 0.06	1.11 ± 0.04
F_X (0.1 – 10 keV) ^c	4.6 ± 0.1	3.7 ± 0.1	6.0 ± 0.2
χ^2_ν/dof	0.94/216	0.90/100	0.93/118
PL + NSA^b			
N_H (10^{20} cm^{-2})	$14.5^{+7.6}_{-7.4}$	$1.8^{+7.2}_{-1.7}$	$10.2^{+7.2}_{-6.1}$
Γ	$1.16^{+0.07}_{-0.08}$	0.98 ± 0.2	$1.04^{+0.10}_{-0.07}$
T_{eff} (10^6 K)	$0.82^{+0.83}_{-0.23}$	$2.73^{+1.40}_{-1.97}$	$1.13^{+1.46}_{-0.51}$
R_{eff} (km)	$0.22^{+5.17}_{-0.22}$	< 0.19	< 1.7
Thermal fraction ^d	0.04 ± 0.05	0.06 ± 0.03	0.07 ± 0.03
F_X (0.1 – 10 keV) ^c	4.8 ± 0.1	3.7 ± 0.1	6.5 ± 0.2
χ^2_ν/dof	0.91/214	0.90/98	0.92/116

^a All uncertainties quoted are 1σ .

^b For the *nsa* model, a $M = 1.4 M_\odot$, $R = 10 \text{ km}$, and $B = 0$ neutron star is assumed. The effective emission radius as measured at the stellar surface, R_{eff} , is calculated assuming the distance range of 1.4 – 3.6 kpc.

^c Unabsorbed X-ray flux (0.1 – 10 keV) in units of $10^{-13} \text{ erg cm}^{-2} \text{ s}^{-1}$.

^d Fraction of unabsorbed flux from the thermal component in the 0.1–10 keV band.

J1023+0038 from a 83-ks observation obtained on 2010 March 24 with *Chandra* ACIS-S (ObsID 11075), when the binary was in an accretion disk-free state (see Bogdanov et al. 2011a, for further details), is shown in the bottom panel of Figure 1. The close similarities between the lightcurves both in morphology and phase alignment are quite striking, further indication that the two systems are close analogs.

4. X-RAY SPECTROSCOPY

4.1. Phase-averaged Spectroscopy

The spectroscopic analysis was carried out in XSPEC⁸ 12.7.1 (Arnaud 1996). Preliminary fits of the individual *XMM-Newton* and *Chandra* spectra produced consistent results so all fits were performed jointly on both data sets to obtain the best constraints on the X-ray spectral properties of XSS J12270–4859. Fitting the phase-averaged spectra with an absorbed power-law results in a statistically acceptable fit (see Table 1 and top panel of Figure 2), with $\chi^2_\nu = 0.94$ for 216 d.o.f., while a single or even a two-temperature neutron star atmosphere thermal spectrum does not yield a satisfactory fit, with $\chi^2_\nu = 2.6$ for 216 d.o.f. and $\chi^2_\nu = 1.6$ for 214 d.o.f., respectively. Since XSS J12270–4859 currently hosts an active rotation-powered pulsar, X-ray-emitting magnetic polar caps heated by a back flow of particles from the pulsar magnetosphere may be present, as seen in many radio MSPs (see, e.g., Zavlin 2006; Bogdanov et al. 2006). Therefore, in addition to the dominant non-thermal emission there may be a non-negligible contribution from the pulsar polar caps. Including the non-magnetic neutron star hydrogen atmosphere *nsa* model (Zavlin et al. 1996) component results in an acceptable fit but the parameters of the thermal component are

⁸ Available at <http://heasarc.nasa.gov/docs/xanadu/xspec/index.html>.

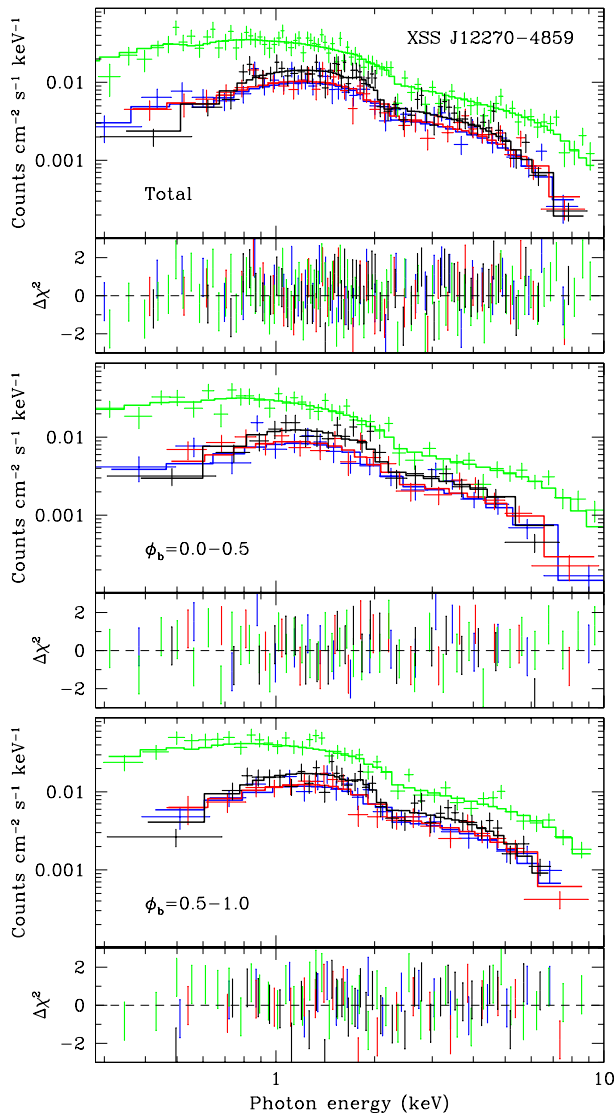


FIG. 2.— *XMM-Newton* EPIC MOS1/2 (red/blue), EPIC pn (green), and *Chandra* ACIS-S (black) phase-averaged X-ray spectra (top) and for orbital phases $\phi_b = 0.0 - 0.5$ (middle) and $\phi_b = 0.5 - 1.0$ (bottom), fitted with an absorbed power-law. The smaller panels show the best-fit residuals in terms of σ with error bars of size one. For the best fit parameters, see text and Table 1.

poorly constrained. The thermal flux contribution is consistent with zero even at a 1σ confidence level and the upper limit on the thermal fraction is $\leq 9\%$.

For both the power-law and composite models, the derived hydrogen column densities along the line of sight, N_H , are in agreement with the value measured through the Galaxy of $\sim 1 \times 10^{21} \text{ cm}^{-2}$ in the direction of XSS J12270–4859 (Kalberla et al. 2005). Assuming the distance range of 1.4–3.6 kpc (de Martino et al. 2013), the derived time-averaged unabsorbed fluxes imply an X-ray luminosity of $(1 - 7) \times 10^{32} \text{ erg s}^{-1}$ in the 0.1–10 keV interval, an order of magnitude fainter than the average luminosity in the accretion disk dominated state.

4.2. Orbital-Phase-resolved Spectroscopy

To look for changes in the X-ray spectrum as a function of the binary orbital phase, we divided the data in two

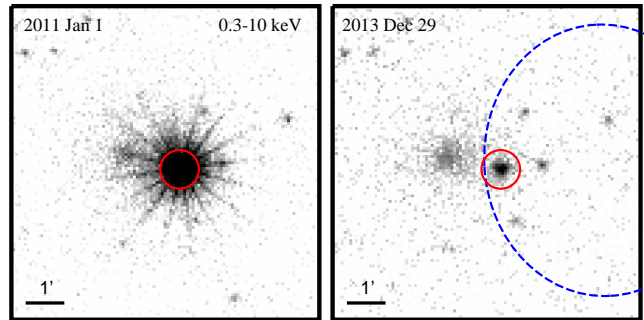


FIG. 3.— *XMM-Newton* EPIC MOS1+2 mosaic images in the 0.3–10 keV band from 2011 Jan 1 (left), during the high state, and 2013 Dec 29 (right), in the current low state of XSS J12270–4859. The red circle of radius $40''$ is centered on the position of XSS J12270–4859. The 95% confidence error ellipse of 2FGL J1227.7–4853 is shown with the dashed blue line. The grayscale shows intensity increasing logarithmically from white to black. North is up and east is to the left.

equal phase portions: $\phi_b = 0.0 - 0.5$ (encompassing the X-ray minimum) and $\phi_b = 0.5 - 1.0$ based on the orbital ephemeris from Bassa et al. (2014). The spectral fits are summarized in columns 3 and 4 of Table 1. An absorbed power-law model yields good fits for both phase intervals (Figure 2) with similar values for the spectral photon index Γ , implying no appreciable spectral variability over the orbit despite the factor of 1.5–1.7 difference in flux. As with the phase-averaged analysis, the addition of an *nsa* model component also results in acceptable fits. For both orbital phase intervals any thermal emission contributes $\lesssim 10\%$ to the 0.1–10 keV flux. The *nsa* temperature and emission radii are poorly constrained but are in general agreement with those observed for thermally-emitting MSPs (e.g., Bogdanov et al. 2006; Zavlin 2006; Bogdanov & Grindlay 2009).

5. X-RAY IMAGING ANALYSIS

Even in its current low state, XSS J12270–4859 still remains the brightest X-ray source in its field. The substantially lower flux allows a close examination of the spatial distribution of emission around the binary for the first time. For XSS J12270–4859, this is especially interesting since a currently active rotation-powered pulsar wind may, in principle interact with circum-binary material that was expelled during the LMXB state via outflows. Moreover, the resulting wind nebula may only be visible for a brief period after the state transition since presumably the material would eventually be swept up by the pulsar wind.

In the most recent images, a diffuse source situated $\sim 1.5'$ east-north-east of XSS J12270–4859 is clearly visible (Figures 3 and 4), which can only barely be seen in the *XMM-Newton* EPIC MOS1+2 image from the high state (2011 January 1) due to the much brighter wings of the point spread function of XSS J12270–4859. The centroid of the diffuse source, which is $\sim 40 - 60''$ in extent, is at approximately $\text{RA} = 12^{\text{h}}28^{\text{m}}07^{\text{s}}.5$ and $\text{Dec} = -48^{\circ}53'24''$ (J2000). To establish if the two objects are associated, we looked for emission connecting XSS J12270–4859 with the extended region by comparing the count rates around XSS J12270–4859 in the direction towards and away from the diffuse source. This was accomplished by consid-

ering a set of adjacent $8''$ by $16''$ rectangular regions aligned along the axis connecting the centroid of the diffuse source and XSS J12270–4859 (see Figure 4). The size was chosen so as to ensure that a sufficient number of photons are collected in each region. Comparing the distribution of counts towards and away from the diffuse region (Figure 5) shows that the emission from the diffuse source does not extend to the position of XSS J12270–4859, suggesting no physical connection between the two X-ray sources.

In addition, if the two objects are in fact associated, the angular separation of $\sim 1.5'$ would translate to a physical separation of $0.6 - 1.6$ pc, and the size of the diffuse region to $0.3 - 1$ pc, for an assumed distance range of $1.4 - 3.6$ kpc. These physical scales are much larger than what is observed in other accreting systems with outflows, such as the microquasars XTE J1550–564 (Kaaret et al. 2003; Tomsick et al. 2003) and H1743–322 (Corbel et al. 2005). Therefore, it is unlikely that the extended emission is a product of an outflow from the binary. Likewise, a pulsar wind nebula (PWN) can be ruled out because XSS J12270–4859 is not embedded in the nebular emission, which also does not resemble a bow shock or a trailing tail (see, e.g., Kargaltsev & Pavlov 2008, for an overview of X-ray PWNe). These factors indicate that an association between the binary and the diffuse source is highly unlikely. It is more likely that the extended object is simply a chance superposition and is unrelated to the binary. Examination of VLT/FORS2 images (3×15 s exposure in R -band obtained on 2010 February 10) show a bright source with morphology resembling that of a galaxy located at $RA=12^h28^m07^s.427$, $Dec.=-48^\circ53'23''.561$ (see bottom panel of Figure 4), which is coincident with the centroid of the diffuse X-ray region and is surrounded by several fainter objects. Therefore, this is likely the central galaxy of a previously uncatalogued galaxy cluster, which we designate as J122807.4–48532, with the diffuse X-ray emission originating from the intra-cluster medium (Cavaliere & Fusco-Fermiano 1976). Additional optical observations are required to conclusively establish this scenario.

The $0.5''$ angular resolution of the ACIS-S image enables an investigation of any nebular emission in the immediate vicinity of the binary (within $\sim 20''$). For this purpose, we have simulated 10 observations of XSS J12270–4859 using ChaRT⁹ and MARX 4.5¹⁰ assuming the parameters of the ACIS-S exposure and the best-fit non-thermal model reported in §4. The mean of the simulated observations was subtracted from the real data to look for excess emission around the binary. However, as apparent from Figure 6, the radial profile of the X-ray emission from XSS J12270–4859 is fully consistent with that of a point source.

We note that this diffuse X-ray source has no radio counterpart in the ATCA image presented by Hill et al. (2011). On the other hand, the eastern component of the radio source designated by Hill et al. (2011) as 1, as well as their source 3, are coincident with very faint X-ray sources (marked in Figure 4). Since these sources are at

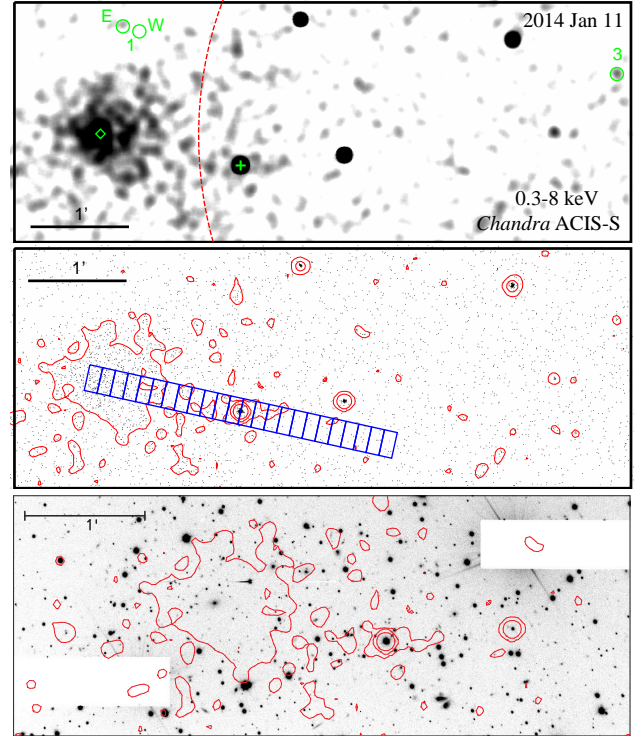


FIG. 4.— *Top*: *Chandra* ACIS-S image in the 0.3–8 keV band from 2014 Jan 11 smoothed with a two-dimensional Gaussian kernel of width $5''$. The green + marks the position of XSS J12270–4859, the green diamond is centered on the optically identified galaxy (see text), and the green circles mark the ATCA radio sources 1 and 3 reported by Hill et al. (2011). The 95% confidence error ellipse of 2FGL J1227.7–4853 is shown with the dashed red line. The grayscale shows intensity increasing logarithmically from white to black. *Middle*: The same image binned at the intrinsic detector resolution of $0.5''$. The red contour levels were obtained from the smoothed image in the top panel. The blue strip of rectangles shows the regions used to extract the count rates shown in Figure 5. Pixel randomization has been removed from the pipeline processing. *Bottom*: VLT/FORS2 image of the field around XSS J12270–4859 with the same X-ray contours shown in the middle panel. Note the extended optical source near the middle of the diffuse X-ray region surrounded by a number of fainter sources.

the threshold of detection in the *Chandra* image, their spectral properties cannot be well constrained.

6. DISCUSSION AND CONCLUSIONS

As reported in Bassa et al. (2014), the recent decline in optical and X-ray brightness and the disappearance of the previously prominent optical emission lines are indicative of the disappearance of the accretion disk in XSS J12270–4859. The *XMM-Newton* and *Chandra* observations of XSS J12270–4859 in its new low flux state presented herein reveal further information regarding this binary:

1. Previously absent large-amplitude modulation at the binary orbital period is now present.
2. The time-averaged X-ray luminosity of $\sim (1 - 7) \times 10^{32}$ erg s $^{-1}$ is smaller by an order of magnitude relative to the accretion disk dominated state.
3. The predominantly non-thermal spectrum with spectral photon index of $\Gamma = 1.2$ is significantly harder than the $\Gamma = 1.7$ observed in the high flux state.
4. The spectral index of the power-law emission ap-

⁹ The *Chandra* Ray Tracer, available at <http://cxc.harvard.edu/soft/ChaRT/cgi-bin/www-saoscac.cgi>

¹⁰ Available at <http://space.mit.edu/cxc/marx/index.html>.

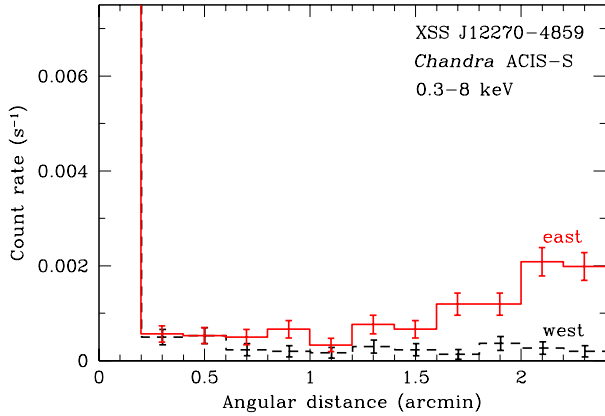


FIG. 5.— Distribution of count rates in the directions towards (east) and away (west) from the nearby diffuse source relative to the centroid of XSS J12270–4859. The count rates were extracted from the rectangular regions depicted in Figure 4.

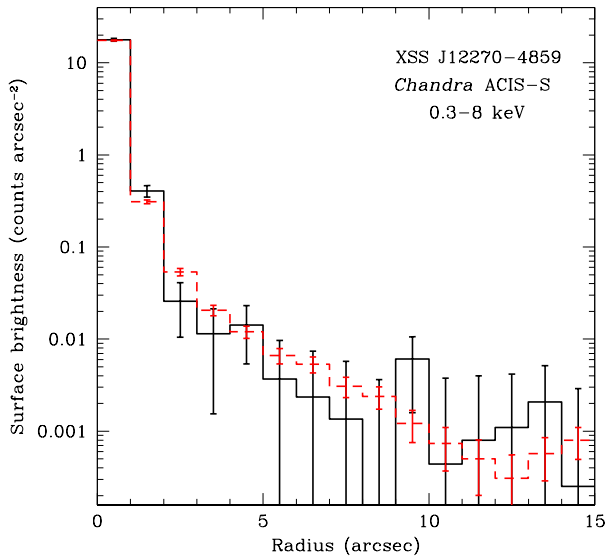


FIG. 6.— Background-subtracted radial profile of XSS J12270–4859 from the *Chandra* ACIS-S observation (black) and a synthetic point spread function generated using ChaRT and MARX (red dashed line).

pears not to vary substantially even though the flux changes by a factor of ~ 1.5 – 1.7 over an orbital period.

These X-ray properties, as well as the optical properties described in Bassa et al. (2014), are identical to what is observed from “redback” radio MSPs, including PSRs J1023+0038 (Archibald et al. 2009, 2010; Bogdanov et al. 2011a), J1723–2837 (Faulkner et al. 2004; Crawford et al. 2013; Bogdanov et al. 2014), J2215+5135 (Hessels et al. 2011; Gentile et al. 2014) in the field of the Galaxy, as well as PSR J0024–7204W in the globular cluster 47 Tuc (Camilo et al. 2000; Freire et al. 2003; Bogdanov et al. 2005), PSR J1740–5340 in NGC 6397 (D’Amico et al. 2001; Bogdanov et al. 2010), and PSR J1824–2452H in M28 (Bogdanov et al. 2011b; Pallanca et al. 2010). Therefore, the results obtained herein, and the recent radio pulsar discovery by Roy et al. (2014) further demonstrate that XSS J12270–4859 is a redback, i.e. a compact binary with an active

rotation-powered pulsar and no accretion disk.

The non-thermal X-rays from redback systems are generated in an intra-binary shock formed by the interaction of the pulsar wind with material from the close companion star (Arons & Tavani 1993). As shown in Bogdanov et al. (2011a), the decline in X-ray flux at $\phi_b \approx 0.25$ seen in PSR J1023+0038 can be reproduced by a simple geometric model in which the intra-binary shock is partially occulted by the bloated secondary star. In this scenario, the depth and phase extent of the X-ray eclipse require that the shock be situated at or very near the surface of the secondary star on the side exposed to the pulsar wind.

There is no indication of extended X-ray emission associated with XSS J12270–4859 that could arise due to outflows in the LMXB phase or the interaction of the pulsar wind with the ambient medium. An adjacent diffuse source is likely not associated with the binary and is probably a background galaxy cluster. Given that only two MSPs, PSRs B1957+21 (Stappers et al. 2003) and J2124–3358 (Hui & Becker 2006) show evidence for X-ray bow shocks, the absence of nebular emission associated with XSS J12270–4859 does not imply the lack of a pulsar wind.

The lack of knowledge of the orbital separation, the companion mass, and the pulsar spin-down luminosity (\dot{E}) for XSS J12270–4859, do not allow meaningful constraints on the physics of the intrabinary shock. Nevertheless, given the nearly identical X-ray properties compared to other redbacks it is possible to place crude constraints on the energetics of the MSP in XSS J12270–4859. In particular, if we consider that the shock luminosity at X-ray maximum is $\sim 2 \times 10^{-3} \dot{E}$ for PSRs J1023+0038 (Archibald et al. 2010; Bogdanov et al. 2011a) and J1723–2837 (Bogdanov et al. 2014), the implied spin-down of the pulsar in XSS J12270–4859 is $(0.7 - 5) \times 10^{35} \text{ erg s}^{-1}$ assuming a distance range 1.4–3.6 kpc. This suggests that the pulsar in XSS J12270–4859 may be among the small number of energetic MSPs with $\dot{E} \gtrsim 10^{35} \text{ erg s}^{-1}$. The 0.1–100 GeV γ -ray luminosity of 2FGL J1227.7–4853, the putative γ -ray counterpart of XSS J12270–4859, of $L_\gamma = (0.8 - 5) \times 10^{34} \text{ erg s}^{-1}$ provides an independent hard lower limit on the \dot{E} of the pulsar, if we assume a γ -ray conversion efficiency of 100%. For efficiencies typical of the MSP population ($\lesssim 50\%$; see Table 10 in Abdo et al. 2013), this yields $\dot{E} \gtrsim 10^{35} \text{ erg s}^{-1}$, in general agreement with the limit obtained from the X-ray luminosity. Continued timing of the radio pulsar would allow a determination of the true \dot{E} of this pulsar.

The redback nature of the XSS J12270–4859 binary determined from the X-ray analysis presented above implies that the pulsar should undergo radio eclipses of frequency-dependent duration around superior conjunction. These eclipses are caused by intra-binary plasma, presumably emanating from the companion star. For most redback and black widow systems that are detectable in radio pulsations, the radio emission is eclipsed for $\lesssim 50\%$ of the orbit, although there is indication that for some systems this fraction can be close to 100% (see Ray et al. 2013, for the case of PSR J1311–3430). The non-detections with the Parkes telescope (Bassa et al.

2014) and only a single, brief detection with the GMRT (Roy et al. 2014) despite deep pulsation searches, are indicative of a high radio eclipse fraction for XSS J12270–4859 that likely varies from orbit to orbit. The large \dot{E} estimated above is consistent with this scenario, since an energetic wind would drive off material from the surface of companion at a higher rate than an MSP with a lower \dot{E} . This may result in occasional severe enshrouding by this stripped material, causing the pulsar to be eclipsed at radio frequencies for a larger fraction of the orbit. This would make XSS J12270–4859 a so-called “hidden” MSP, as postulated by Tavani (1991).

The X-ray properties of XSS J12270–4859 in both the present disk-free radio pulsar state and the accretion disk-dominated state (see de Martino et al. 2010, 2013) are virtually identical to those of PSRs J1023+0038 (Archibald et al. 2010; Bogdanov et al. 2011a; Patruno et al. 2014) and J1824–2452I (Papitto et al. 2013; Linares et al. 2014). This remarkable consistency in X-ray characteristics provides a powerful discriminant for identifying more such MSP binaries, especially

ones that are heavily enshrouded and hence cannot be identified via radio pulsation searches.

A.M.A. and J.W.T.H. acknowledge support from a Vrije Competitie grant from NWO. C.B. acknowledges support from ERC Advanced Grant “LEAP” (227947, PI: Michael Kramer). J.W.T.H. and A.P. acknowledge support from NWO Vidi grants. J.W.T.H. also acknowledges funding from an ERC Starting Grant “DRAG-NET” (337062). A portion of the results presented was based on observations obtained with *XMM-Newton*, an ESA science mission with instruments and contributions directly funded by ESA Member States and NASA. The scientific results reported in this article are based in part on observations made by the *Chandra X-ray Observatory*. This research has made use of the NASA Astrophysics Data System (ADS), software provided by the Chandra X-ray Center (CXC) in the application package CIAO.

Facilities: *XMM, CXO*

REFERENCES

- Alpar, M. A., Cheng, A. F., M. A. Ruderman, M. A., & Shaham, J. 1982, *Nature*, 300, 728
- Abdo, A. A., et al. 2013, *ApJS*, 208, 17
- Archibald, A. M., et al. 2009, *Science*, 324, 1411
- Archibald, A. M., Kaspi, V. M., Bogdanov, S., et al. 2010, *ApJ*, 722, 88
- Arnaud, K. A. 1996, in *ASP Conf. Ser. 101, Astronomical Data Analysis Software and Systems V*, ed. G. H. Jacoby & J. Barnes (San Francisco, CA: ASP), 17
- Arons, J. & Tavani M. 1993, *ApJ*, 403, 249
- Backer, D. C., Kulkarni, S. R., Heiles, C., Davis, M. M., Goss, W. M. 1982, *Nature*, 300, 615
- Bassa, C. G., Patruno, A., Hessels, J. W. T., et al. 2014, *MNRAS*, 441, 1825
- Bogdanov, S., Grindlay, J. E., & van den Berg, M. 2005, *ApJ*, 630, 1029
- Bogdanov, S., Grindlay, J. E., Heinke, C. O., Camilo, F., Freire, P. C. C., & Becker, W. 2006, *ApJ*, 646, 1104
- Bogdanov, S. & Grindlay, J. E. 2009, *ApJ*, 703, 1557
- Bogdanov, S., van den Berg, M., Heinke, C. O., Cohn, H. N., Lugger, P. M., Grindlay, J. E. 2010, *ApJ*, 709, 241
- Bogdanov, S., Archibald, A. M., Hessels, J. W. T., et al. 2011a, *ApJ*, 742, 97
- Bogdanov, S., van den Berg, M., Servillat, M., et al. 2011b, *ApJ*, 730, 81
- Bogdanov, S., Esposito, P., Crawford, F., Possenti, A., McLaughlin, M. A., Freire, P. 2014, *ApJ*, 781, 6
- Butters, O. W., Norton, A. J., Hakala, P., Mukai, K., Barlow, E. J. 2008, *A&A*, 487, 271
- Camilo, F., Lorimer, D. R., Freire, P., Lyne, A. G., & Manchester, R. N. 2000, *ApJ*, 535, 975
- Corbel, S., Kaaret, P., Fender, R. P., Tzioumis, A. K., Tomsick, J. A., Orosz, J. A. 2005, *ApJ*, 632, 504
- Cavaliere, A., & Fusco-Femiano, R. 1976, *A&A*, 49, 137
- Crawford, F., Lyne, A. G., Stairs, I. H., et al. 2013, *ApJ*, 776, 20
- D’Amico, N., Lyne, A. G., Manchester, R. N., Possenti, A., & Camilo, F. 2001, *ApJ*, 548, L171
- de Martino, D., Belloni, T., Falanga, M., et al. 2013, *A&A*, 550, 89
- de Martino, D., Falanga, M., Bonnet-Bidaud, J.-M., et al. 2010, *A&A*, 515, 25
- Donati, J.-F., & Landstreet, J. D., *ARA&A*, 47, 333
- Faulkner, A. J., Stairs, I. H., Kramer, M., et al. 2004, *MNRAS*, 355, 147
- Freire, P. C., Camilo, F., Kramer, M., Lorimer, D. R., Lyne, A. G., Manchester, R. N., & D’Amico, N. 2003, *MNRAS*, 340, 1359
- Fruchter, A. S., Stinebring, D. R., & Taylor, J. H. 1988, *Nature*, 333, 237
- Fruscione, A., McDowell, J. C., Allen, G. F., et al. 2006, *Proc. SPIE*, 6270, 62701V
- Gentile, P., Roberts, M., McLaughlin, M., et al. 2014, *ApJ*, 783, 69
- Hessels, J. W. T., Roberts, M. S. E., McLaughlin, M. A., et al. 2011, in *AIP Conf. Proc. 1357, Radio Pulsars: an Astrophysical Key to Unlock the Secrets of the Universe*, ed. M. Burgay et al. (Melville, NY: AIP), 40
- Hill, A. B., Szostek, A., Corbel, S., et al. 2011, *MNRAS*, 415, 235
- Hui, C. Y., & Becker, W. 2006, *A&A*, 448, L13
- Kaaret, P., Corbel, S., Tomsick, J. A., Fender, R., Miller, J. M., Orosz, J. A., Tzioumis, A. K., Wijnands, R. 2003, *ApJ*, 582, 945
- Kalberla, P. M. W., Burton, W. B., Hartmann, D., Arnal, E. M., Bajaja, E., Morras, R., Pöppel, W. G. L. 2005, *A&A*, 440, 775
- Kargaltsev, O., & Pavlov, G. G. 2008, in *AIP Conf. Proc. 983, 40 Years of Pulsars: Millisecond Pulsars, Magnetars and More*, ed. C. G. Bassa, Z. Wang, A. Cumming, & V. M. Kaspi (Melville, NY: AIP), 171
- Linares, M., Bahramian, A., Heinke, C., Wijnands, R., Patruno, A., Altamirano, D., Homan, J., Bogdanov, S., Pooley, D. 2014, *MNRAS*, 438, 251
- Masetti, N., Morelli, L., Palazzi, E., et al. 2006, *A&A*, 459, 21
- Nolan, P. L., Abdo, A. A., Ackermann, M., et al. 2012, *ApJS*, 199, 31
- Pallanca, C., Dalessandro, E., Ferraro, F. R., et al. 2010, *ApJ*, 725, 1165
- Paltani, S. 2004, *A&A*, 420, 789
- Papitto, A., Ferrigno, C., Bozzo, E., et al. 2013, *Nature*, 501, 517
- Papitto, A., Torres, D. F., Li, J. 2014, *MNRAS*, 438, 2105
- Patruno, A., Archibald, A. M., Hessels, J. W. T., et al. 2014, *ApJ*, 781, L3
- Patruno, A., & Watts, A. L. to appear in “Timing neutron stars: pulsations, oscillations and explosions”, T. Belloni, M. Mendez, C. M. Zhang Eds., *ASSL*, Springer
- Pretorius, M. L. 2009, *MNRAS*, 395, 386
- Radhakrishnan, V., & Srinivasan, G. 1982, *Science*, 51, 1096
- Ray, P. S., Ransom, S. M., Cheung, C. C., et al. 2013, *ApJ*, 763, L13
- Roy, J., Bhattacharyya, B., Ray, P. S. 2014, *The Astronomer’s Telegram*, 5890, 1
- Roberts, M. S. E. 2011, in *AIP Conf. Ser. 1357, Radio Pulsars: An Astrophysical Key to Unlock the Secrets of the Universe*, ed. M. Burgay, N. D’Amico, P. Esposito, A. Pellizzoni, & A. Possenti (Melville, NY: AIP), 127
- Stappers, B. W., Bailes, M., Lyne, A. G., et al. 1996, *ApJ*, 465, L119
- Stappers, B. W., Gaensler, B. M., Kaspi, V. M., van der Klis, M., & Lewin, W. H. G. 2003, *Science*, 299, 1372
- Stappers, B. W., Archibald, A. M., Hessels, J. W. T., et al. 2014, *ApJ*, in press (eprint arXiv:1311.7506)
- Strüder, L. et al. 2001, *A&A*, 365, L18
- Tavani, M. 1991, *ApJ*, 379, L69
- Tendulkar, S. P., Yang, C., An, H., et al. 2014, *ApJ*, submitted
- Thorstensen, J. R. & Armstrong, E. 2005, *AJ*, 130, 759
- Turner, M. J. L. 2001, *A&A*, 365, L27
- Tomsick, J. A., Corbel, S., Fender, R., et al. 2003, *ApJ*, 582, 933
- Wang, Z., Archibald, A. M., Thorstensen, J. R., Kaspi, V. M., Lorimer, D. R., Stairs, I., Ransom, S. M. 2009, *ApJ*, 703, 2017

Wijnands, R., & van der Klis, M. 1998, *Nature*, 394, 344
Zavlin, V. E., Pavlov, G. G., & Shibano, Yu. A. 1996, *A&A*, 315,
141

Zavlin, V. E. 2006, *ApJ*, 638, 951